Kinetic Approach to Quasi-Ballistic Field-Dependent Electron Transport

A. R. St.Denis[1] and D. L. Pulfrey[2]
[1]Nortel Networks, Nepean, Ontario K2H8E9, Canada
[2]Department of Electrical and Computer Engineering,
University of British Columbia, Vancouver, BC V6T1Z4, Canada

Abstract. An accurate description of electron transport in small-dimension semiconductor devices demands that the Boltzmann Transport Equation (BTE) be rigorously solved. Further, because critical regions in transistors, such as graded bases or short channels, are not field-free, it is necessary to consider the problem of field-dependent transport. In this work, we present a kinetic approach based on the concept of path integrals which provides an exact solution to the BTE for electron transport in regions where a uniform electric field is present.

1. Introduction

Carrier transport in regions of modern semiconductor devices that have feature sizes of the order of a mean-free-path length can be studied via the semi-classical Boltzmann Transport Equation (BTE). The base region of heterojunction bipolar transistors is a case in point, and quantum features, such as tunneling from the emitter, can be included in the solution to the BTE via appropriate boundary conditions [1]. A convenient method of solving the implicit integral relation for the electron distribution in a small region of semiconductor is the iterative approach of Grinberg and Luryi [2], which casts the problem in a set of two differential equations, one each for the forward- and backward-directed fluxes in a one-dimensional problem. This method has been applied in the field-free case to both elastic- [2] and inelastic- [1] scattering mechanisms. Application to regions in which there is an electric field is complicated by the forward- and backward-directed fluxes becoming coupled by the field and, therefore, the components of the two fluxes are not as easily described.

Here we visualize the various components (ballistic and scattered) of the forward- and backward-directed fluxes via a kinetic approach. This allows the path integrals for the components to be readily defined. For the case of isotropic, elastic scattering in a uniform field, the equations are in a form that allows solution by the iterative method previously described [1, 2]. Such a case is examined in this paper, and the components of the electron distribution are identified and described for various injection levels, field strengths and region widths.

2. Kinetic Approach to Transport

Consider a situation in which the electron distribution function is inhomogeneous only in the distance coordinate z, *i.e.*, $f(\vec{r},\vec{k}) = f(z,k,\theta)$, where θ is the angle between the wavevector of magnitude k and the z-axis. The essence of the kinetic approach to transport is the intuitive determination of the different ways a carrier can come to be at some position z. In general, there are two such ways: one involving ballistic transport directly to z from the injecting boundary, and the other involving some number of collisions before arriving at z. Thus,

$$f(z,k,\theta) = f_{\mathrm{BAL}}(z,k,\theta) + f_{\mathrm{COL}}(z,k,\theta). \tag{1}$$

Further, the distribution function itself can be split into forward- and backward- (positive- and negative-z-directed) components, f^+ and f^- respectively, each with its own ballistic and collision constituents.

To derive the ballistic component in the forward-going ensemble, for example, note that in the absence of an electric field

$$f^+_{\mathrm{BAL}}(z,k,\theta) = f^+(0,k,\theta)P(z), \tag{2}$$

where $P(z)$ is the probability that a carrier injected at $z=0$ travels to z without suffering a collision. For further travel to $z+dz$ at a velocity v_z,

$$P(z+dz) = P(z)\left[1 - \frac{dz}{v_z\tau}\right], \tag{3}$$

where $1/\tau$ is the collision rate. Expanding (3), solving for $P(z)$ and noting that $P(0)=1$ gives

$$P(z) = \exp\left[-\int_0^z \frac{d\xi}{v_z\tau}\right]. \tag{4}$$

Substituting into (2) gives the general result for the ballistic component of the forward-going ensemble:

$$f^+_{\mathrm{BAL}}(z,k,\theta) = f^+(0,k,\theta)\exp\left[-\int_0^z \frac{d\xi}{v_z\tau}\right]. \tag{5}$$

For the collision component of the forward-going ensemble, the number of carriers that have scattered into f at some $z=z'$ in the time interval dt and remain within dz' of z' is $v_z^{-1}\mathcal{C}_{\mathrm{in}}(z')dz'$, where $\mathcal{C}_{\mathrm{in}}$ is the incoming collision integral. Following the procedure used for the ballistic component, the number of these which reach z without suffering another collision is

$$f^+_{\mathrm{COL}}(z,k,\theta) = \int_0^z \frac{\mathcal{C}_{\mathrm{in}}(z')}{v_z}\exp\left[-\int_{z'}^z \frac{d\xi}{v_z\tau}\right]dz'. \tag{6}$$

The ballistic and collision components of the backward-going ensemble can be developed in an analogous fashion. Extension to field-dependent transport requires only that (5) and (6) be modified to account for the resulting change of $\vec{k}$ with position.

2.1. The uniform-field case

The kinetic approach is intuitive and general, and can be applied to regions with arbitrary potential distributions [3]. Here we consider the specific case of electron transport in a region of width W in which there is a uniform electric field $\mathcal{E}$. Specifically, the electric field is taken to be negative, so the field tends to push electrons from left to right, *i.e.*, the direction referred to as forward in this paper. Conservation of total energy requires that

$$k(z') = \sqrt{k^2 - a(z - z')}\,, \tag{7}$$

where

$$a = \frac{2m}{\hbar^2} q|\mathcal{E}| \quad \equiv \quad \frac{2m}{\hbar^2}\frac{V(0) - V(z)}{z}\,, \tag{8}$$

with V being the potential energy. The corresponding angle between the wavevector and the z-axis is

$$\theta^{\pm}(z') = \cos^{-1}\left(\pm\sqrt{\frac{k^2\cos^2\theta - a(z - z')}{k^2 - a(z - z')}}\right)\,, \tag{9}$$

where the $\pm$ label indicates forward- or backward-going motion, respectively, *i.e.*, $0 \leq \theta < 90$ for forward-going, and $90 < \theta \leq 180$ for negative-going. Further, in a one-dimensional potential such as that being considered here, the perpendicular component of the wavevector, $k_\perp$, is conserved. Therefore, the longitudinal component can be written as

$$k_z^{\pm}(z') = \pm\sqrt{k_z(z)^2 - a(z - z')}\,. \tag{10}$$

2.1.1. Forward components The trajectories labelled f^+ in Fig. 1 show the ways in which a carrier can come to be in the forward-going distribution at some point z. Note that there are two significant features introduced by the presence of the field. Firstly, carriers injected from the boundary at W can be turned from the backward-going component into the forward-going component by the potential. This coupling of the forward- and backward- going components does not exist in the field-free case, where the collision integrals provide the only coupling between the counter-directed parts of the distribution [1]. Secondly, the potential profile allows carriers which reach z to have a kinetic energy which differs from that which they possessed at their injecting boundary.

The part of the ballistic component of the forward-going ensemble injected at $z = 0$ follows directly from (5):

$$f^+_{\mathrm{BAL},1}(z, k, \theta) = f^+(0, k_0, \theta_0)\exp\left[-\int_0^z \frac{d\xi}{v_z^+\tau}\right]\,, \quad \text{for } k^2\cos^2\theta > az, \tag{11}$$

where $k_0 = \sqrt{k^2 - az}\,,\quad v_z^+\tau = v_z(k_z^+(\xi))\tau(k(\xi))$ and

$$\theta_0 = \cos^{-1}\left(\sqrt{\frac{k^2\cos^2\theta - az}{k^2 - az}}\right)\,.$$

$f^+_{\mathrm{BAL},2}$, the other contribution to the ballistic component, comes from those electrons that are injected at $z = W$ and are turned around by the potential at the reflection point $z = \zeta$. This component does not include those carriers injected at W with enough z-directed kinetic energy to surmount the full potential barrier and which reach $z = 0$

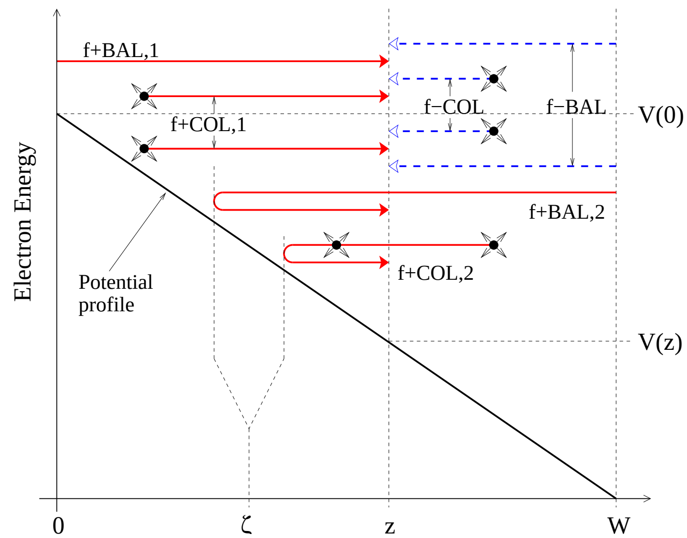

Figure 1. A schematic of the means by which electrons can come to be in the distribution at some point z, when a linear potential energy profile is present. The trajectories represent carrier paths, with the 'star' indicating a scattering site at $z = z'$. The vertical distance between the trajectories and the potential energy profile represents the z-directed kinetic energy of the carrier. Two contributions to each of $f^+_{COL,1}$, f^-_{COL} and f^-_{BAL} are shown to indicate that these components can have total energies above and below V(0).

ballistically, as these carriers are absorbed at the left boundary. Thus, the reflected electrons have $\hbar^2 k_z(z)^2 < 2m[V(0) - V(z)]$, and must have been injected at $z = W$ with a z-component which follows from (10), namely:

$$k_z(W) = -\sqrt{k_z^2 + a(W - z)}\ . \tag{12}$$

The number that reach z after being turned around by the potential at a reflection point ζ is then obtained by multiplying by the probability a carrier travels from W to ζ, and then back to z, without suffering a collision. Thus, analogously to (11):

$$f^+_{\mathrm{BAL},2}(z,k,\theta) = f^-(W,k_W,\theta_W)\exp\left[-\left(\int_W^\zeta \frac{d\xi}{v_z^-\tau} + \int_\zeta^z \frac{d\xi}{v_z^+\tau}\right)\right], \quad \text{if } k^2\cos^2\theta < az, \tag{13}$$

where $k_W = \sqrt{k^2 + a(W - z)}$, $\quad v_z^-\tau = v_z(k_z^-(\xi))\tau(k(\xi))$ and

$$\theta_W = \cos^{-1}\left(-\sqrt{\frac{k^2\cos^2\theta + a(W - z)}{k^2 + a(W - z)}}\right)\ ,\quad \zeta = z - \frac{k^2\cos^2\theta}{a}\ .$$

For the collision components of the forward-going distribution, we distinguish between two cases on the basis of the direction of the carrier after its last collision at z', prior to arriving at z.

Firstly, carriers scattered to the left of z into the forward-going direction can proceed directly to z. For this instance, it follows directly from (6) that:

$$f^+_{\mathrm{COL},1}(z,k,\theta) = \int_0^z \frac{\mathcal{C}_{\mathrm{in}}(z',k(z'),\theta^+(z'))}{v_z^+(z')}\exp\left[-\int_{z'}^z \frac{d\xi}{v_z^+\tau}\right]dz', \quad \text{for } k^2\cos^2\theta > 0, \tag{14}$$

where $v_z^+(z') = v_z(k_z^+(z'))$.

Secondly, a carrier with a z-directed kinetic energy such that $0 < \hbar^2 k_z^2(z) < 2m[V(0) - V(z)]$ can collide into a backward-going state anywhere between ζ and W and be reflected by the potential barrier into a forward-going state. Two possible collision sites are indicated in Fig. 1. The prescription for this component is:

$$f^+_{\mathrm{COL},2}(z,k,\theta) = \int_W^\zeta \frac{\mathcal{C}_{\mathrm{in}}(z', k(z')\theta^-(z'))}{v_z^-(z')} \exp\left[-\left(\int_{z'}^\zeta \frac{d\xi}{v_z^-\tau} + \int_\zeta^z \frac{d\xi}{v_z^+\tau}\right)\right] dz' \quad \text{if } k^2\cos^2\theta < az \;, \tag{15}$$

where $v_z^-(z') = v_z(k_z^-(z'))$.

2.1.2. Backward components The ways in which a carrier can come to be in the backward-going distribution are not complicated by the possibility of reflection, so their descriptions follow directly from the negative-going analogs of (5) and (6), *i.e.*,

$$f^-_{\mathrm{BAL}}(z,k,\theta) = f^-(W, k_W, \theta_W) \exp\left[-\left(\int_W^z \frac{d\xi}{v_z^-\tau}\right)\right], \tag{16}$$

and

$$f^-_{\mathrm{COL}}(z,k,\theta) = \int_W^z \frac{\mathcal{C}_{\mathrm{in}}(z', k(z'), \theta^-(z'))}{v_z^-(z')} \exp\left[-\left(\int_{z'}^z \frac{d\xi}{v_z^-\tau}\right)\right] dz' \;. \tag{17}$$

3. Solution for Elastic and Isotropic Scattering

The precise scattering mechanisms involved in the transport process enter into the preceding equations via the incoming collision integral $\mathcal{C}_{\mathrm{in}}$ and the collision rate τ. Here, only scattering that is both isotropic and elastic is accounted for, such as would be the case when acoustic phonon scattering is dominant. The lifetime and incoming collision integral for such a situation can then be cast in simple forms [2], *i.e.*:

$$\tau = \frac{1}{\alpha_{\mathrm{ap}} k} \;\text{ and }\; \mathcal{C}_{\mathrm{in}} = \alpha_{\mathrm{ap}} k \frac{1}{2} \int_0^\pi f(z,k,\theta) d\theta \;. \tag{18}$$

This lifetime leads to a mean free path length of

$$l_{\mathrm{sc}} = v\tau = \frac{\hbar}{\alpha_{\mathrm{ap}} m}. \tag{19}$$

Substituting these expressions into (11, 13, 14, 15, 16, 17) defines the set of equations that must be solved to achieve a solution to the BTE. These equations were solved numerically using an iterative procedure analogous to that used in the field-free situation described elsewhere [1].

4. Results and Discussion

As a particular example of the application of the transport equations derived via the kinetic approach, we consider quasi-ballistic transport in a region for which the injected fluxes, $f^+(0,k,\theta)$ and $f^-(W,k,\theta)$, are considered to be hemi-Maxwellians, then:

$$f^+(0,k_0,\theta_0) = \frac{n_{\mathrm{E}}^*}{N_c} e^{-\eta(k^2 - az)} \;\text{ and }\; f^-(W,k_W,\theta_W) = \frac{n_{\mathrm{C}}^*}{N_c} e^{-\eta(k^2 + a(W-z))} \tag{20}$$

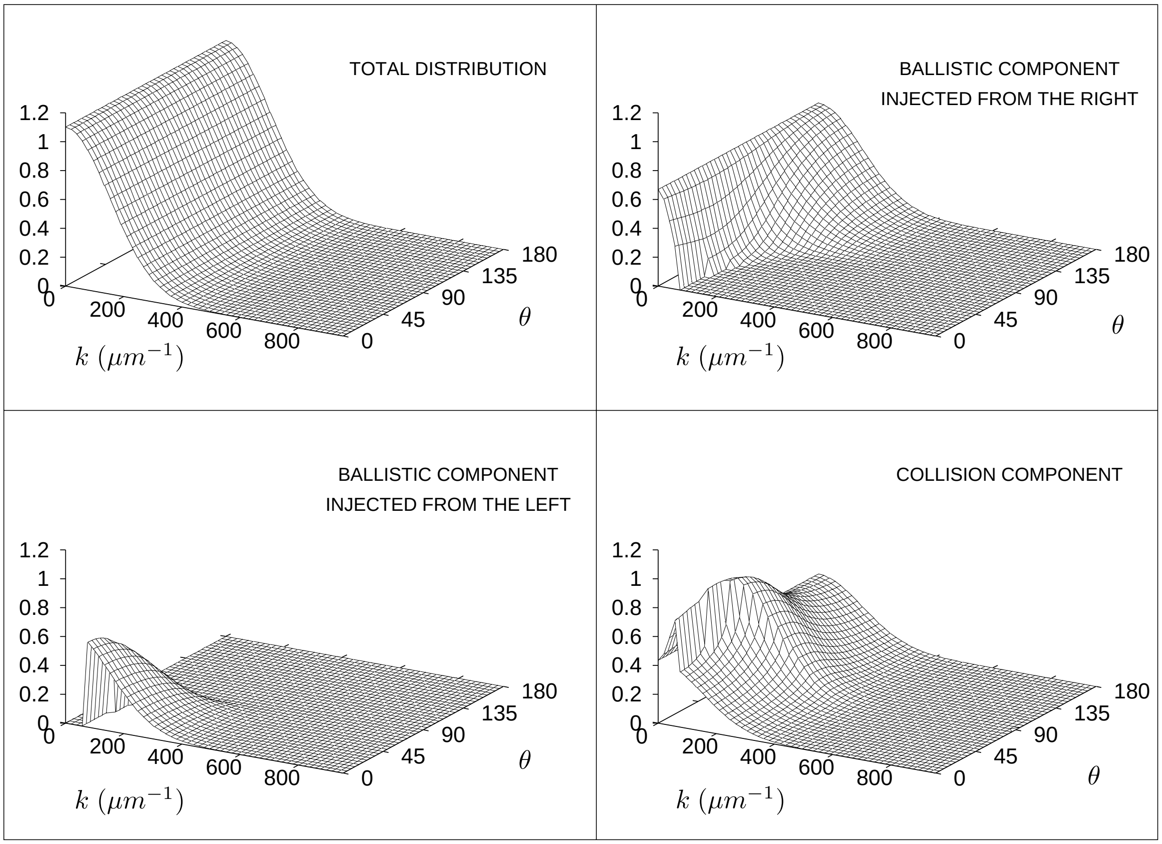

Figure 2. The full equilibrium distribution (forward and backward fluxes), along with its ballistic and collision components, at the middle of a region with field strength $\mathcal{E} = 10^5 V/m$ and width $W = l_{\rm sc}$.

where $\eta = \hbar^2/2m\mathrm{k_B}T$, with k_B being the Boltzmann constant; N_c is the effective density of states in the conduction band of the injecting semiconductor regions; $n^*_{\rm E}/2$ and $n^*_{\rm C}/2$ are the carrier concentrations in the fluxes injected from the left and the right, respectively [2]. Such a situation could arise, for example, in the compositionally graded base region of a bipolar transistor or in a Mott barrier. Only low and moderate field strengths are examined, since the restriction on the collision integrals to elastic scattering cannot describe the velocity saturation effect occurring at high electric fields.

4.1. The equilibrium picture

The full equilibrium distribution , *i.e.*, the forward and backward ensembles along with their ballistic and collision components, is shown in Figure 2 at the mid-point of a region with $W = l_{sc}$ and $\mathcal{E} = 10^5 V/m$. In this, and subsequent plots, the distribution is normalized to the peak value of f at $z = 0$. The total equilibrium distribution is, of course, an appropriately weighted Maxwellian. The ballistic and collision components, however, exhibit a number of interesting features. Consider first the ballistic component injected from the right. For the backward-going part of this component (*i.e.*, $90 < \theta < 180$, corresponding to $f^-_{\rm BAL}$ in Fig. 1), notice how as θ gets closer to 90, the distribution falls off. This is because such carriers see an effectively longer path than those directed more closely along the z-axis. For the forward-going part of this component (*i.e.*, $0 < \theta < 90$), notice that the component vanishes for $k^2 \cos^2 \theta > az$. This is because ballistic carriers that have been injected from the right and subsequently turned into forward-going carriers by the field cannot have a z-component of wave vector such that $k_z^2 > az$ (see the trajectory corresponding to $f^+_{\mathrm{BAL},2}$ in Fig. 1). Ballistic carriers with a z-directed component of wave vector such that $k_z^2 > az$ must appear in the component injected from the left ($f^+_{\mathrm{BAL},1}$ in Fig. 1), as shown in the lower left of Figure 2. Note that for carriers with $k_z^2 < az$ this component is non-existent, and for angles closer to 90, the longer effective path length once again causes the distribution to fall off more rapidly than for angles closer to 0.

Consider now the collision component. Notice how there appears to be a depression of the forward-going part of this component where $k^2 \cos^2 \theta > az$. This occurs because, as consideration of Figure 1 indicates, there is an effectively shorter path over which carriers can collide into appropriate states to end up with $k_z^2 > az$ at z, than to end up with $k_z^2 < az$. At equilibrium this is of course balanced by the ballistic component $f^+_{BAL,1}$ to yield the Maxwellian shape of the equilibrium distribution. This depression gets less pronounced if the distribution is examined closer to W, *i.e.*, after more collisions have occurred.

4.2. The non-equilibrium case

To obtain a net electron flow in the forward direction, the flux injected from the left is increased beyond its equilibrium value, while that injected from the right is maintained at its equilibrium value. For n^*_{E} greater than about 10 times the equilibrium value $\bar{n}^*_{\mathrm{E}}$, the flux from the left is overwhelmingly dominant, and the normalized distribution becomes independent of further increases in the level of injection from the left [3]. The following results are for the case in which $n^*_{\mathrm{E}} = 10^5 \times \bar{n}^*_{\mathrm{E}}$.

The dependence of the distribution on field strength, at the middle of a region with $W = 2 \times l_{\mathrm{sc}}$, is shown in Figure 3. At $\mathcal{E} = 10^4 V/m$ the displacement of the distribution along the k-axis has become noticeable, and this trend continues to become more pronounced as the field strength is further increased. This is simply a manifestation of the potential energy difference between $z = 0$ and $z = W/2$ increasing with increasing field strength.

Another interesting trend is that the distribution becomes more closely focused about the z-axis as the field strength is increased. This is because it is only k_z that is increased more by the higher fields, while $k_\perp$ remains unchanged by the field. Finally, note the size of the distribution is decreasing with increasing field strength. This is because as the field increases the speed of the carriers, it must also rarefy their density in order to maintain a constant current density across the region.

With respect to the distribution in the bottom-left frame of Fig. 3, the distribution becomes more concentrated in the domain of $k_z^2 > az$ as the regional width is reduced, due to the increasing dominance of the ballistic component. As the region width gets larger, carriers travel a larger distance to reach the middle of the region. They thereby undergo more collisions, leading to a decrease in the importance of the ballistic component and a corresponding increase in the collision component. Thus, there is a trend to a more angularly uniform shape of the distribution as the region width is increased.

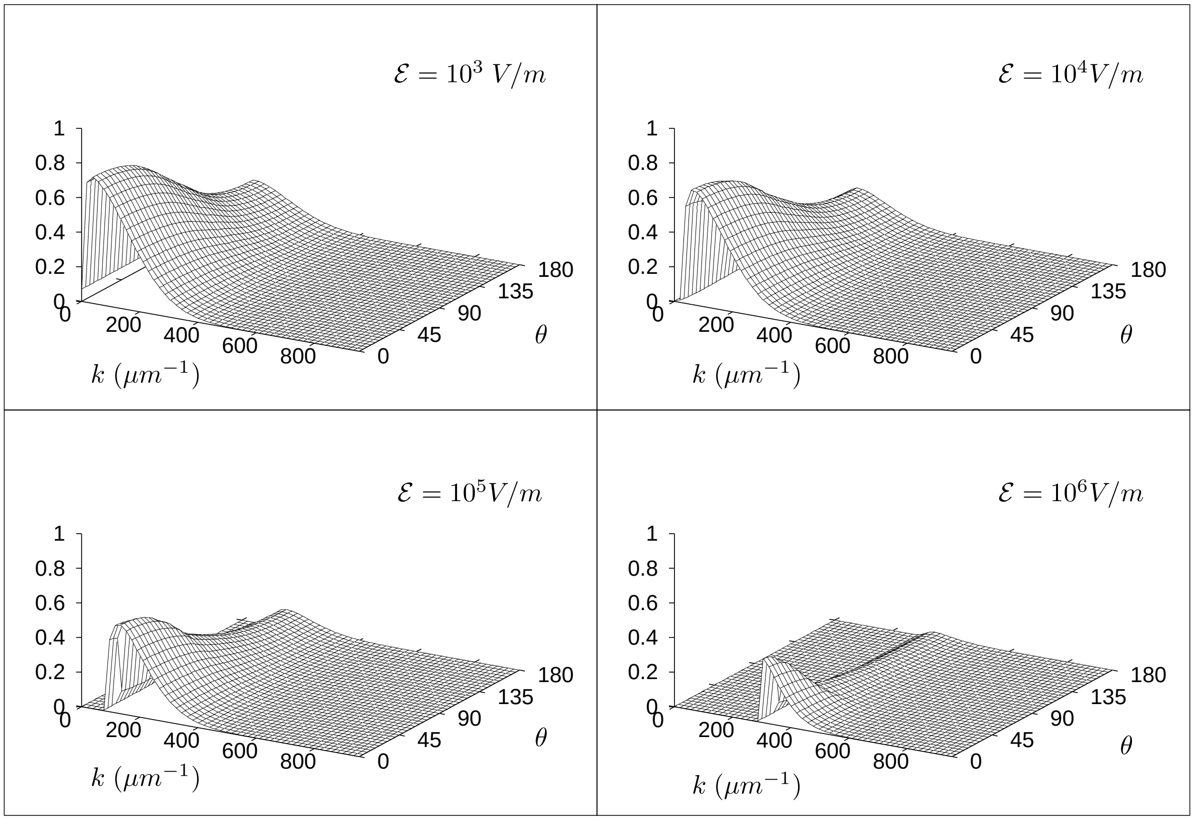

Figure 3. The field-strength dependence of the full distribution, at the middle of a region with width $W = 2 \times l_{\rm sc}$ and an injection level of $n^*_{\rm E} = 10^5 \times \bar{n}^*_{\rm E}$.

5. Conclusions

It can be concluded that the kinetic approach offers an intuitive and convenient way of forming the path-integral relations that describe the quasi-ballistic transport of electrons in short semiconductor regions subjected to a uniform electric field. The ballistic and collision components of the electron ensemble are readily characterized and, in this work where acoustic-phonon scattering is considered, both components are evident, even for transport in regions as short as one mean-free-path length and with fields as high as 10^5 V/m. The information that is revealed on the energy and angular dependence of the distribution allows new insight into the field dependence of macroscopic properties of the ensemble, such as mobility [3, 4].

References

[1] St.Denis A R and Pulfrey D L 1998 J. Appl. Phys. 84 4959-4965
[2] Grinberg A A and Luryi S 1992 Solid-State Electron. 35 1299-1309
[3] St.Denis A R 1999 Ph.D. thesis (University of British Columbia)
[4] St.Denis A R, Vaidyanathan M and Pulfrey D L 2002 IEEE Trans. Electron Dev. (to be submitted)